The 8th European Congress on Computational Methods in Applied Sciences and Engineering
ECCOMAS Congress 2022
5-–9 June 2022, Oslo, Norway

AN ENERGY-PRESERVING UNCONDITIONALLY STABLE FRACTIONAL STEP METHOD ON COLLOCATED GRIDS

D. SANTOS, F. X. TRIAS, G. COLOMER, C. D. PÉREZ-SEGARRA

[1]Heat and Mass Transfer Technological Center, Technical University of Catalonia
Carrer de Colom 11, 08222 Terrassa (Barcelona), Spain. www.cttc.upc.edu
{daniel.santos.serrano, francesc.xavier.trias, guillem.colomer, cdavid.perez.segarra}@upc.edu

Key words: FVM, energy-preserving, symmetry-preserving, unconditionally stable, FSM, collocated

Abstract. Preservation of energy is fundamental in order to avoid the introduction of unphysical energy that can lead to unstable simulations. In this work, an energy-preserving unconditionally stable fractional step method on collocated grids is presented as a method which guarantees both preservation of energy and stability of our simulation. Using an algebraic (matrix-vector) representation of the classical incompressible Navier-Stokes equations mimicking the continuous properties of the differential operators, conservation of energy is formally proven. Furthermore, the appearence of unphysical velocities in highly distorted meshes is also adressed. This problem comes from the interpolation of the pressure gradient from faces to cells in the velocity correction equation, and can be corrected by using a proper interpolation.

1 INTRODUCTION

The Navier-Stokes equations are the basic equations that describe mass and momentum conservation in fluid dynamics. A general solution for these equations is not known, so many different numerical methods were developed in order to obtain numerical approximations. A widely used family of numerical methods applied to fluid dynamics are the Finite Volume Methods. Many general purpose CFD codes, such as OpenFOAM or ANSYS-Fluent, use a finite volume method in order to discretise the equations and obtain numerical solutions over unstructured meshes. A collocated arrangement is used by these codes due to its simplicity and its computational cost[1, 2], in spite of a staggered configuration seems to be the natural arrangement of the discrete unknowns of our discretised equations [3, 4, 5].

Furthermore, these codes use stencil formulations, that is, once the equations are discretized, an algorithm run cell by cell computing the desired quantities. In contrast, algebraic formulations maintain the equations in matrix-vector form, and compute the required quantities by using these matrices and vectors.

One possible method to solve the velocity-pressure coupling is the classical fractional step method [6, 7, 8]. However, using a collocated framework and a wide stencil Poisson equation in such a method lead us to the well-known checkerboard problem. This problem can be solved by means of working with a compact stencil Poisson equation [9, 10] or by regularizing

of the convective term such as [1].

Many problems or unstabilities can be found in the numerical solution of these equations. Namely, conservation of energy is fundamental in order to obtain numerical solutions, because introduction of unphysical energy can lead us to unstable simulations. Furthermore, from our point of view, it is crucial to respect the physical structure of the equations in order to obtain reliable solutions. Respecting the (continuous) symmetries of the differential operators will allow us to conserve energy. This conservation is naturally achieved by means of mimicking the continuous properties, and it is no longer imposed by conservation arguments.

Another common problem is the appearence of unphysical velocities in highly distorted meshes. These spurious velocities come from the interpolation from faces to cells of the discrete pressure gradient. Many reconstructions of the discrete gradient have been proposed [11, 12, 13, 14]. However, they do not usually respect the underlying symmetries of the continuos gradient and divergence operator. In this work, stability of the solution is guaranteed by means of respectig the symmetries of the continuous gradient and divergence operator, which give us a particular construction of the discrete gradient operator, in terms of the discrete divergence.

Finally, it is worth to mention that some popular open-source codes such as OpenFOAM introduces a large amount of numerical dissipation to the simulations [15]. In our opinion, this is not appropiate since this artificial dissipation interferes with the subtle balance between convective transport and physical dissipation, in addition to distort the effect of the model in LES simulations. Hence, reliable numerical methods for DNS/LES must be free of numerical dissipation (or, at least, have an small amount), and, of course, unconditionally stable, i.e. simulations must be stable regardless of the mesh quality and resolution.

The paper is arranged as follows. A symmetry-preserving finite volume discretization on collocated grids of the Navier-Stokes equations is presented in section 2, where conservation of energy is also discussed. Section 3 addresses the stability of the pressure gradient interpolation in the velocity correction equation. Finally, section 4 presents a numerical example in order to show the stability of the method.

2 SYMMETRY-PRESERVING FINITE VOLUME DISCRETIZATION ON COLLOCATED GRIDS

The dimensionless Navier-Stokes equations for Newtonian and incompressible flows in primitive variables are

$$\frac{\partial \boldsymbol{u}}{\partial t} + (\boldsymbol{u}\cdot\nabla)\,\boldsymbol{u} = \frac{1}{Re}\Delta\boldsymbol{u} - \nabla p, \tag{1a}$$

$$\nabla\cdot\boldsymbol{u} = 0, \tag{1b}$$

where Re is the dimensionless Reynolds number. A fully-conservative finite-volume discretization respecting the symmetries of the differential operators for structured and unstructured meshes on collocated grids was presented in [1]. Assuming n control volumes and m faces:

$$\Omega\frac{d\boldsymbol{u}_c}{dt} + \mathsf{C}\left(\boldsymbol{u}_s\right)\boldsymbol{u}_c + \mathsf{D}\boldsymbol{u}_c + \Omega\mathsf{G}_c\boldsymbol{p}_c = \boldsymbol{0}_c, \tag{2a}$$

$$\mathsf{M}\boldsymbol{u}_s = \boldsymbol{0}_c, \tag{2b}$$

where $\boldsymbol{p}_c = (p_1, p_2, \ldots, p_n)^T \in \mathbb{R}^n$ and $\boldsymbol{u}_c \in \mathbb{R}^{3n}$ are the cell-centered pressure and velocity fields. The subindices c and s refer to whether the variables are cell-centered or staggered at the faces. For simplicity $\boldsymbol{u}_c$ is defined as a column vector and arranged as $\boldsymbol{u}_c = (\boldsymbol{u}_1, \boldsymbol{u}_2, \boldsymbol{u}_3)^T$, where $\boldsymbol{u}_i = \Big((u_i)_1, (u_i)_2, \ldots, (u_i)_n\Big)^T$ are the vectors containing the velocity components corresponding to the x_i-spatial direction. In order to assure mass conservation in the control volumes, a secondary velocity field is defined at the faces $\boldsymbol{u}_s = \Big((u_s)_1, (u_s)_2, (u_s)_3, \ldots, (u_s)_m\Big)^T \in \mathbb{R}^m$. Variables defined at cells and at faces are related via a linear shift interpolator from cells to faces $\Gamma_{c\to s} \in \mathbb{R}^{m\times 3n}$. Both velocities can be related as follows

$$\boldsymbol{u}_s \equiv \Gamma_{c\to s}\boldsymbol{u}_c. \tag{3}$$

The matrices $\Omega \in \mathbb{R}^{3n\times 3n}$, $\mathsf{C}\left(\boldsymbol{u}_s\right) \in \mathbb{R}^{3n\times 3n}$ and $\mathsf{D} \in \mathbb{R}^{3n\times 3n}$ are block diagonal matrices given by

$$\Omega = \mathsf{I}_3 \otimes \Omega_c, \qquad \mathsf{C}\left(\boldsymbol{u}_s\right) = \mathsf{I}_3 \otimes \mathsf{C}_c\left(\boldsymbol{u}_s\right), \qquad \mathsf{D} = \mathsf{I}_3 \otimes \mathsf{D}_c, \tag{4}$$

where $\mathsf{I}_3 \in \mathbb{R}^{3\times 3}$ is the identity matrix and $\Omega_c \in \mathbb{R}^{n\times n}$ is a diagonal matrix with the cell-centered control volumes. $\mathsf{C}_c\left(\boldsymbol{u}_s\right) \in \mathbb{R}^{n\times n}$ and $\mathsf{D}_c \in \mathbb{R}^{n\times n}$ are the cell-centered convective and diffusive operators for a discrete scalar field, respectively. Finally, $\mathsf{G}_c \in \mathbb{R}^{3n\times n}$ represents the discrete gradient operator and the matrix $\mathsf{M} \in \mathbb{R}^{n\times m}$ is the face-to-center discrete divergence operator.

The volumetric interpolator from cells to faces $\Gamma_{c\to s}$ can be constructed by means of two matrices: the scalar cell-to-face interpolator, $\Pi_{c\to s} \in \mathbb{R}^{m\times n}$, and $N = (N_{s,x}N_{s,y}N_{s,z}) \in \mathbb{R}^{3m\times m}$, where $N_{s,i} \in \mathbb{R}^{m\times m}$ is a diagonal matrix containing the x_i spatial components of the face normal vectors:

$$\Gamma_{c\to s} = N(\mathsf{I}_3 \otimes \Pi_{c\to s}). \tag{5}$$

In this formulation, all the operators needed to write the equations can be constructed using only five discrete ones: the cell-centered and staggered control volumes (diagonal matrices), Ω_c and Ω_s, the face normal vectors, N_s, the scalar cell-to-face interpolation, $\Pi_{c\to s}$ and the cell-to-face divergence operator, M. Notice that Ω_c, Ω_s and N_s are given by the geometry of the mesh, while $\Pi_{c\to s}$ can be freely chosen. Due to its simplicity, it makes a code build within this framework to be easily portable [16, 17].

2.1 Conservation of energy and constraint on the shift operator

The discrete inner-product is defined as follows:

$$< \boldsymbol{v}_c, \boldsymbol{u}_c >= \boldsymbol{v}_c^T \Omega \boldsymbol{u}_c, \tag{6}$$

so the global discrete kinetic energy can be computed as $||\boldsymbol{u}_c||^2 \equiv \boldsymbol{u}_c^T \Omega \boldsymbol{u}_c$. Its temporal evolution equation can be obtained by left-multiplying Eq. (2a) by $\boldsymbol{u}_c^T$ and summing the resulting expression with its transpose

$$\begin{aligned} \frac{d}{dt}||\boldsymbol{u}_c||^2 &= -\boldsymbol{u}_c^T \left(\mathsf{C}\left(\boldsymbol{u}_s\right) + \mathsf{C}\left(\boldsymbol{u}_s\right)^T \right) \boldsymbol{u}_c - \boldsymbol{u}_c^T \left(\mathsf{D} + \mathsf{D}^T \right) \boldsymbol{u}_c \\ & -\boldsymbol{u}_c^T \Omega \mathsf{G}_c \boldsymbol{p}_c - \boldsymbol{p}_c^T \mathsf{G}_c^T \Omega^T \boldsymbol{u}_c. \end{aligned} \tag{7}$$

In absence of diffusion ($\mathsf{D} = 0$) the global kinetic energy $||\boldsymbol{u}_c||^2$ is conserved if:

$$\mathsf{C}\left(\boldsymbol{u}_s\right) = -\mathsf{C}\left(\boldsymbol{u}_s\right)^T, \tag{8a}$$

$$-\left(\Omega \mathsf{G}_c\right)^T = \mathsf{M}\Gamma_{c\to s}. \tag{8b}$$

One can impose these restrictions from a physical point of view, in purpose of conservation of energy. However, there are mathematical reasons in order to fulfill these restrictions. Given two vectorial spaces, A and B, a continuous operator T, a discretization operator π_h, we can construct the diagram shown in Figure 1, being A_h, B_h and T_h the discrete counterparts of the continuous spaces and operator:

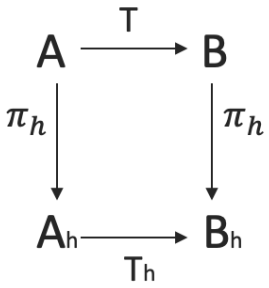

Figure 1: Diagram between vectorial spaces and their discrete counterparts. We will require this diagram to be commutative.

If we assume this diagram to be commutative, T_h is going to retain (or mimick) the continuous properties of T. Recalling that the gradient operator is the adjoint operator of the divergence:

$$< \nabla \cdot a | b >= - < a | \nabla b >, \tag{9}$$

where $< a|b >= \int_\Omega abdV$ represents the inner product of functions, we can now discretise these quantities by means of π_h:

$$< \Omega_1^{-1} M a_h | b_h >_{\Omega_1} = - < a_h | G b_h >_{\Omega_2} . \tag{10}$$

If $\Omega_1 = \Omega$ and $\Omega_2 = \Omega_s$, which is the case in the collocated formulation, then:

$$G = -\Omega_s^{-1} M^T. \tag{11}$$

In contrast, if all the variables are located in the cell-center, $\Omega_1 = \Omega$ and $\Omega_2 = \Omega$ and defining $\Gamma_{s\to c} \in \mathbb{R}^{3n\times m}$ as the (volumetric) interpolator from faces to cells:

$$< \Omega_1^{-1} M \Gamma_{c\to s} a_h | b_h >_{\Omega} = - < a_h | \Gamma_{s\to c} G b_h >_{\Omega}, \tag{12}$$

and developing this expression we obtain the desired result:

$$-\left(\Omega \mathsf{G}_c\right)^T = \mathsf{M}\Gamma_{c\to s}. \tag{13}$$

Furthermore, combining (11) and (13) we obtain a constraint for the shift operators:

$$\left(\Omega\Gamma_{s\to c}\Omega_s^{-1}\mathsf{M}^T\right)^T = \mathsf{M}\Gamma_{c\to s} \longrightarrow \Gamma_{s\to c} = \Omega^{-1}\Gamma_{c\to s}^T\Omega_s, \tag{14}$$

Finally, from the skew-symmetry of the continuos convective operator follows that $\mathsf{C}\left(\boldsymbol{u}_s\right)$ should be a skew-symmetric matrix.

In our opinion, mathematical arguments are preferred over physical impositions, since conservation of energy is obtained in a natural way by mimicking the underlying symmetries of the continuous operators, but the conversely is not true, and as it has been proven here, all the constraints presented in [1] follow from the simpler assumption that the previous diagram should be commutative.

2.2 Solving the pressure-velocity coupling. Checkerboard problem

Semidiscretized momentum equation (2a) can be rewritten as follows

$$\frac{d\boldsymbol{u}_c}{dt} = \mathsf{R}\left(\boldsymbol{u}_c\right) - \mathsf{G}_c\boldsymbol{p}_c, \tag{15}$$

where $\mathsf{R}\left(\boldsymbol{u}_c\right) \equiv -\Omega^{-1}\left(\mathsf{C}\left(\boldsymbol{u}_s\right)\boldsymbol{u}_c + \mathsf{D}\boldsymbol{u}_c\right)$. For the temporal discretization, a fully explicit scheme is assumed whereas the incompressibility constraint is treated implicitly. Introducing the functions f and $\mathbf{R}$, which represent a general fully explicit discretization, the fully-discretized NS equations read

$$\begin{aligned} \mathsf{M}\boldsymbol{u}_s^{n+1} &= \mathbf{0}_c, \\ \frac{f(\boldsymbol{u}_c^{n+1},...,\boldsymbol{u}_c^0)}{\Delta t} &= \mathbf{R}(\boldsymbol{u}_c^n,...,\boldsymbol{u}_c^0) - \mathsf{G}_c\boldsymbol{p}_c^{n+1}. \end{aligned} \tag{16a}$$

The simplest case would be a first-order forward Euler: $f(\boldsymbol{u}_c^{n+1},...,\boldsymbol{u}_c^0) = \boldsymbol{u}_c^{n+1} - \boldsymbol{u}_c^n$.

To solve the velocity-pressure coupling, a classical fractional step method [6, 7, 8] is used. For the staggered velocity field, $\boldsymbol{u}_s$, this projection is derived from the Helmholtz-Hodge vector decomposition theorem [18], whereby a velocity $\boldsymbol{u}_s^p$ can be uniquely decomposed into a solenoidal vector, $\boldsymbol{u}_s^{n+1}$, and a curl-free vector, expressed as the gradient of a scalar field, $\mathsf{G}\tilde{\boldsymbol{p}}_c{}'$. This decomposition is written as

$$\boldsymbol{u}_s^p = \boldsymbol{u}_s^{n+1} + \mathsf{G}\tilde{\boldsymbol{p}}_c{}'. \tag{17}$$

Then, taking the divergence of Eq.(17) yields a discrete Poisson equation for $\tilde{\boldsymbol{p}}_c{}'$

$$\mathsf{M}\boldsymbol{u}_s^p = \mathsf{M}\boldsymbol{u}_s^{n+1} + \mathsf{MG}\tilde{\boldsymbol{p}}_c{}' \quad \longrightarrow \quad \mathsf{MG}\tilde{\boldsymbol{p}}_c{}' = \mathsf{M}\boldsymbol{u}_s^p. \tag{18}$$

Finally, using the definition of G given in Eq.(11) the previous equation becomes

$$\mathsf{L}\tilde{\boldsymbol{p}}_c{}' = \mathsf{M}\boldsymbol{u}_s^p \qquad \text{with} \qquad \mathsf{L} \equiv -\mathsf{M}\Omega_s^{-1}\mathsf{M}^T, \tag{19}$$

where the discrete compact Laplacian operator $\mathsf{L} \in \mathbb{R}^{n\times n}$ is, by construction, a symmetric negative-definite matrix. Once the solution is obtained, $\boldsymbol{u}_s^{n+1}$ results from the correction (17)

$$\boldsymbol{u}_s^{n+1} = \boldsymbol{u}_s^p - \mathsf{G}\tilde{\boldsymbol{p}}_c{}'. \tag{20}$$

3 STABILITY OF THE PRESSURE GRADIENT INTERPOLATION

In order to illustrate the procedure, let us assume a first-order forward Euler temporal scheme. The cell-centered velocity at time step n can be computed recursively as follows:

$$\begin{aligned}
\boldsymbol{u}_c^n &= \boldsymbol{u}_c^p - \mathsf{G}_c\tilde{\boldsymbol{p}}_c{}' = \boldsymbol{u}_c^{n-1} + \Delta t^n \mathsf{R}\left(\boldsymbol{u}_c^{n-1}\right) - \mathsf{G}_c(\tilde{\boldsymbol{p}}_c{}^p + \tilde{\boldsymbol{p}}_c{}') = \\
&= \left(\boldsymbol{u}_c^{n-2} + \Delta t^{n-1}\mathsf{R}\left(\boldsymbol{u}_c^{n-2}\right) - \mathsf{G}_c\tilde{\boldsymbol{p}}_c{}^{n-1}\right) + \Delta t^n \mathsf{R}\left(\boldsymbol{u}_c^{n-1}\right) - \mathsf{G}_c\tilde{\boldsymbol{p}}_c{}^n = \ldots = \\
&= \boldsymbol{u}_c^0 + \sum_{i=1}^{n} \Delta t^i \mathsf{R}\left(\boldsymbol{u}_c^{i-1}\right) - \mathsf{G}_c \sum_{i=0}^{n} \tilde{\boldsymbol{p}}_c{}^i.
\end{aligned} \tag{21}$$

Introducing it in the Poisson equation leads to:

$$\begin{aligned}
\mathsf{L}\tilde{\boldsymbol{p}}_c{}^{n+1} &= \mathsf{M}_c\boldsymbol{u}_c^n + \Delta t^{n+1}\mathsf{M}_c\mathbf{R}^n - (\mathsf{L}-\mathsf{L}_c)\tilde{\boldsymbol{p}}_c{}^p = \\
&= \mathsf{M}_c\boldsymbol{u}_c^0 + \mathsf{M}_c\sum_{i=1}^{n+1}\Delta t^i \mathsf{R}\left(\boldsymbol{u}_c^{i-1}\right) - \mathsf{L}_c\sum_{i=0}^{n}\tilde{\boldsymbol{p}}_c{}^i + (\mathsf{L}-\mathsf{L}_c)\tilde{\boldsymbol{p}}_c{}^p.
\end{aligned} \tag{22}$$

Here, $\mathsf{L}_c = \mathsf{M}_c\mathsf{G}_c \in \mathbb{R}^{n\times n}$ is the wide-stencil collocated Laplacian. Now, we can define $\bar{\boldsymbol{p}}_c{}^n = \sum_{i=0}^{n}\tilde{\boldsymbol{p}}_c{}^i$. Observe that $\tilde{\boldsymbol{p}}_c{}^{n+1} = \bar{\boldsymbol{p}}_c{}^{n+1} - \bar{\boldsymbol{p}}_c{}^n$. This allows us to rearrange the previous equation as:

$$\mathsf{L}\bar{\boldsymbol{p}}_c{}^{n+1} = \mathsf{M}_c\boldsymbol{u}_c^0 + \mathsf{M}_c\sum_{i=1}^{n+1}\Delta t^i \mathsf{R}\left(\boldsymbol{u}_c^{i-1}\right) + (\mathsf{L}-\mathsf{L}_c)\bar{\boldsymbol{p}}_c{}^n + (\mathsf{L}-\mathsf{L}_c)\tilde{\boldsymbol{p}}_c{}^p. \tag{23}$$

This can be viewed as a stationary iterative solver. The stability of this process will depend on the eigenvalues of $\mathsf{L}^{-1}\mathsf{L}_c$ and $(\mathsf{L}-\mathsf{L}_c)$.

Inverting L , let us define $\mathsf{T_1} = \mathsf{L}^{-1}(\mathsf{L}-\mathsf{L}_c)$ and $\mathsf{T_2} = \mathsf{L}^{-1}\mathsf{L}_c$. If $\mu_i^{\mathsf{T}_1}$ and $\mu_i^{\mathsf{T}_2}$ are their eigenvalues, the process will converge if $|\mu_i^{\mathsf{T}_1}| < 1$ and $|\mu_i^{\mathsf{T}_2}| < 1$.
Notice that

$$\mathsf{L}^{-1}(\mathsf{L}-\mathsf{L}_c) = \mathsf{I} - \mathsf{L}^{-1}\mathsf{L}_c \implies \mu_i^{\mathsf{T}_1} = 1 - \mu_i^{\mathsf{T}_2}. \tag{24}$$

$\mathsf{L}^{-1}\mathsf{L}_c$ is the product of two negative definite matrices so $\mathsf{L}^{-1}\mathsf{L}_c$ is a positive definite matrix. Thus, $\mu_i^{\mathsf{T}_1} = 1 - \mu_i^{\mathsf{T}_2} < 1$ (we impose it in order to reach convergence).
On the other hand, if $\mathsf{L}-\mathsf{L}_c$ is negative definite, then $\mathsf{L}^{-1}(\mathsf{L}-\mathsf{L}_c)$ is positive definite, so $\mu_i^{\mathsf{T}_1} > 0$.
We can conclude that $\mu_i^{\mathsf{T}_1} \in (0,1)$ and it implies that $\mu_i^{\mathsf{T}_2} \in (0,1)$ and the process converge.
In conclusion, we have to study the definiteness of $\mathsf{L}-\mathsf{L}_c$, that depends in the geometry and interpolator as follows:

$$\begin{aligned} \mathsf{L}-\mathsf{L}_c &= -\mathsf{M}\Omega_s^{-1}\mathsf{M}^T + \mathsf{M}\Gamma_{c\to s}\Omega^{-1}\Gamma_{c\to s}^T\mathsf{M}^T \\ &= -\mathsf{M}(\Omega_s^{-1} - \Gamma_{c\to s}\Omega^{-1}\Gamma_{c\to s}^T)\mathsf{M}^T. \end{aligned} \tag{25}$$

So, in order to conclude that $\mathsf{L}-\mathsf{L}_c$ is negative definite, we need $\Omega_s^{-1} - \Gamma_{c\to s}\Omega^{-1}\Gamma_{c\to s}^T$ to be negative definite.

This problem was more generally adressed in [19] for any kind of explicit scheme and it was proven that for Cartesian meshes and their stretchings, a volume weighted interpolator will make our system of equations to be stable. The volume weighted interpolator can be constructed as follows:

$$\Pi_{c\to s} = \Delta_s^{-1}\Delta_{sc}^T, \tag{26}$$

where $\Delta_s \in \mathbb{R}^{m\times m}$ is a diagonal matrix containing the projected distances between two adjacent control volumes, and $\Delta_{sc} \in \mathbb{R}^{m\times n}$ is a matrix containing the projected distances between an adjacent cell node and its corresponding face. Figure 2 shows a representation of these distances.

We have strong reasons to think that this interpolator is also stable for general unstructured meshes. However, a formal prove has not been found yet. To illustrate this fact, next section will present a numerical case with a highly distorted mesh.

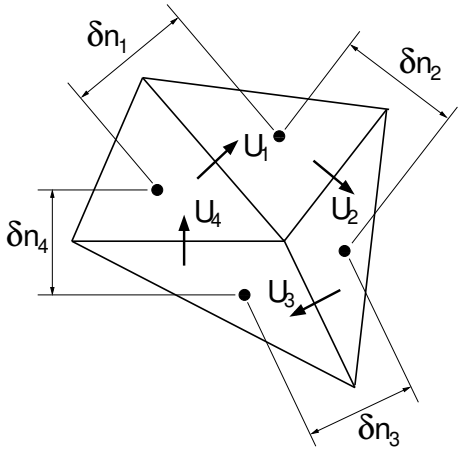

Figure 2: δn_i are the components of Δ_s, while the components of Δ_{sc} would be calculated in the same way but taking the distance between a control volume and their corresponding face centers.

4 AIR-FILLED DIFFERENTIALLY HEATED CAVITY FOR EXTREMELY DISTORTED UNSTRUCTURED MESHES

In order to check the stability of the method, some tests have been carried out with very coarse and very bad quality meshes. Here, a differentially heated cavity test is presented:

- Air-filled (Pr = 0.71).
- Height-to-width aspect ratio 2.
- Rayleigh number (based on the cavity height) of 10^6.

The mesh used to run the case is shown in Figure 3:

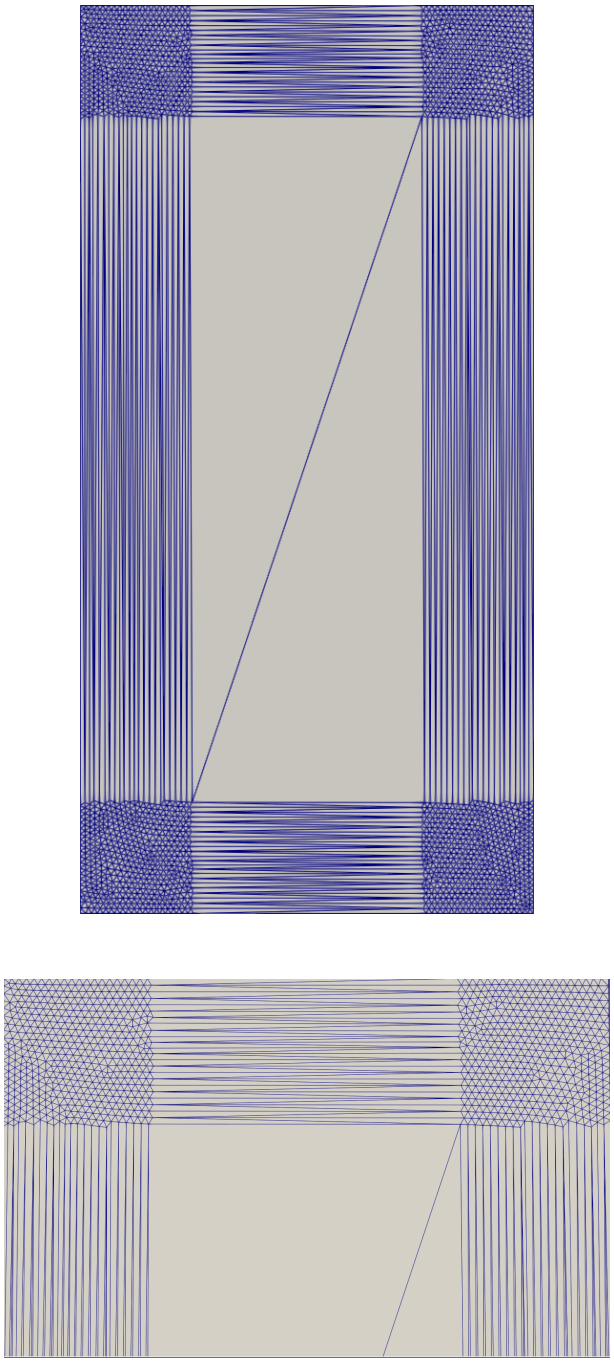

Figure 3: (Top) Highly distorted mesh used to run the case. (Bottom) Zoom of the top part of the mesh.

The results for this case are shown in Figures 4, 5, 6 and 7:

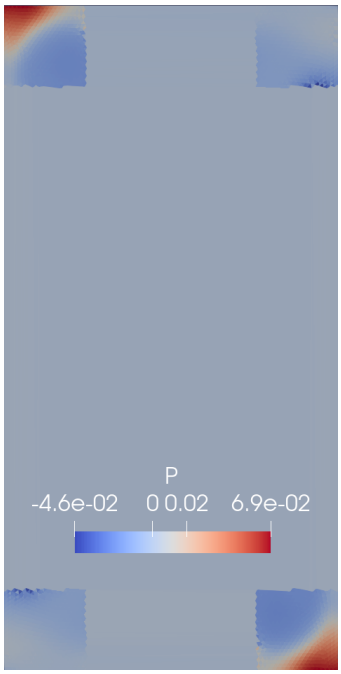

Figure 4: Pressure distribution obtained for the test mesh shown in Figure 3.

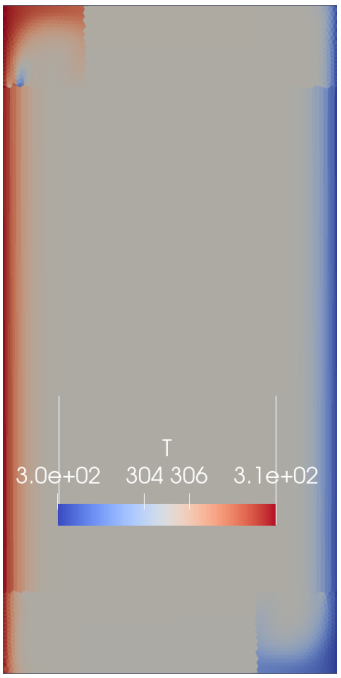

Figure 5: Temperature distribution obtained for the test mesh shown in Figure 3.

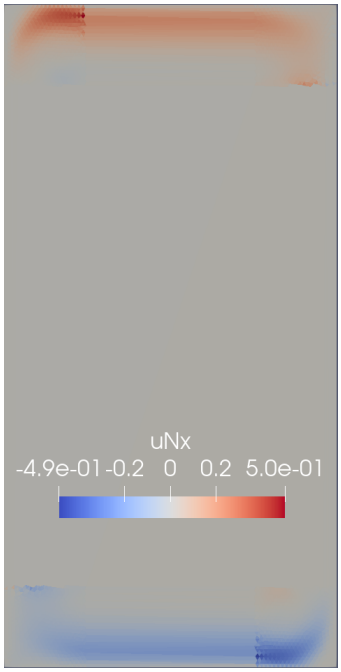

Figure 6: Velocity in x direction obtained for the test mesh shown in Figure 3.

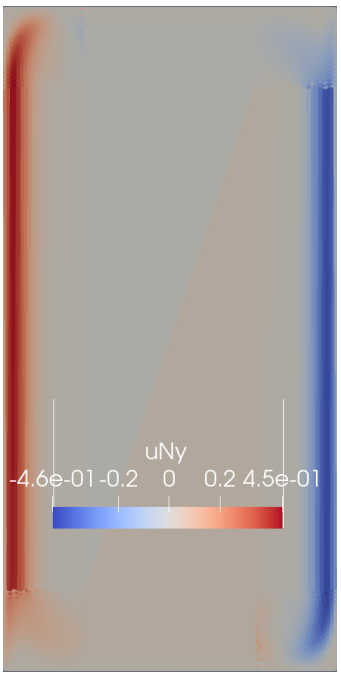

Figure 7: Velocity in y direction obtained for the test mesh shown in Figure 3.

It is worth to mention that interpolating the pressure gradient with other interpolation schemes, such as a mid-point scheme, will blow up the simulation from the first iterations.

5 CONCLUSIONS AND FUTURE WORK

In this work an energy-preserving unconditionally stable fractional step method has been presented. This work continues the one started in [1] by Trias et. al., giving mathematical support to some relations assumed in order to preserve energy, and reducing the degree of freedom for choosing the interpolation from faces to cells of the pressure gradient, in order to achieve stability. With the volume weighted interpolator the stability is guaranteed for Cartesian meshes, while for general unstructured meshes the problem remains opened. However, numerical tests for highly distorted unstructured triangular meshes are fully stable.
The future work regarding the method goes in two lines. The first line is to prove theoretically the stability for general unstructured meshes. The second line will be to test accuracy of the method, and in particular, test the accuracy of the volume weighted interpolator for the pressure gradient.

Acknowledgments

This work has been financially supported by the project RETOtwin [PDC2021-120970-I00] funded by MCIN/AEI/10.13039/501100011033 and European Union Next Generation EU/PRTR. D. Santos acknowledges a *FI AGAUR-Generalitat de Catalunya* fellowship (2020FI_B_00839). The authors thankfully acknowledge these institutions.

REFERENCES

[1] F. X. Trias, O. Lehmkuhl, A. Oliva, C.D. Pérez-Segarra, and R.W.C.P. Verstappen. Symmetry-preserving discretization of Navier-Stokes equations on collocated unstructured meshes. *Journal of Computational Physics*, 258:246–267, 2014.

[2] A. Pascau. Cell face velocity alternatives in a structured colocated grid for the unsteady Navier-Stokes equations. *International Journal for Numerical Methods in Fluids*, 65:812–833, 2011.

[3] F. Harlow and J. Welch. Numerical calculation of time-dependent viscous incompressible flow of fluid with free surface. *The Physics of Fluids*, 8(12):2182–2189, 1965.

[4] R. Verstappen and A. Veldman. Symmetry-preserving discretization of turbulent flow. *Journal of Computational Physics*, 187:343–368, 2003.

[5] F. Ham, F. Lien, A. Strong. A fully conservative second-order finitie difference scheme for incompressible flow on nonuniform grids. *Journal of Computational Physics*, 177(1):117–133, 2002.

[6] A. J. Chorin. Numerical Solution of the Navier-Stokes Equations. *Mathematics of Computation*, 22:745–762, 1968.

[7] N. N. Yanenko. *The Method of Fractional Steps*. Springer-Verlag, 1971.

[8] J. B. Perot. An analysis of the fractional step method. *Journal of Computational Physics*, 108:51–58, 1993.

[9] C. M. Rhie and W. L. Chow. Numerical study of the turbulent flow past an airfoil with trailing edge separation. *AIAA Journal*, 21(11):1525–1532, 1983.

[10] C. M. Klaij. On the stabilization of finite volume methods with co-located variables for incompressible flow. *Journal of Computational Physics*, 297:84–89, 2015.

[11] B. Diskin and J. Thomas. Accuracy of gradient reconstruction on grids with high aspect ratio. *NIA Report*, (2008-12), 2009.

[12] A. Syrakos, S. Varchanis, Y. Dimakopoulos, A. Goulas and J. Tsamopoulous. A critical analysis of some popular methods for the discretisation of the gradient operator in finite volume methods. *Physics of Fluids*, 29, 2017.

[13] M. Deka, S. Brahmachary, R. Thirumalaisamy, A. Dalal and G. Natarajan. A new Green–Gauss reconstruction on unstructured meshes. Part I: Gradient reconstruction. *Journal of Computational Physics*, 422, 2020.

[14] A. Katz and V. Sankaran. High aspect ratio grid effects on the accuracy of navier–stokes solutions on unstructured meshes. *Computers Fluids*, (65):66–79, 2012.

[15] E.M.J. Komen, L.H. Camilo, A. Shams, B.J. Geurts, B. Koren. A quantification method for numerical dissipation in quasi-DNS and under-resolved DNS, and effects of numerical dissipation in quasi-DNS and under-resolved DNS of turbulent channel flows. 345:565–595, 2017.

[16] X. Álvarez, A. Gorobets, F.X. Trias. A hierarchical parallel implementation for heterogeneous computing. Application to algebra-based CFD simulations on hybrid supercomputers. *Computers Fluids*, 214:104768, 2021.

[17] E. Komen, J.A. Hopman, E.M.A. Frederix, F.X. Trias, and R.W.C.P Verstappen. A symmetry-preserving second-order timeaccurate PISO-based method. *Computers Fluids*, 225:104979, 2021.

[18] A. J. Chorin and J. E. Marsden. *A Mathematical Introduction to Fluid Mechanics*. Springer, third edition, 2000.

[19] D. Santos, J. Muela, N. Valle, F. Trias. On the Interpolation Problem for the Poisson Equation on Collocated Meshes. *14th WCCM-ECCOMAS Congress 2020*.